

1 **Tempo-spatial variation of the late Mesozoic volcanism in Southeast**
2 **China**

3 Xianghui Li^{1, 2 *}, Yongxiang Li¹, Jingyu Wang¹, Chaokai Zhang¹, Yin Wang³, Ling Liu³
4

5 ¹State Key Laboratory for Mineral Deposits Research, School of Earth Sciences and Engineering, Nanjing University,
6 Nanjing 210023 China

7 ²State Key Laboratory of Oil and Gas Reservoir Geology and Exploitation, Chengdu University of Technology, Chengdu
8 610059, China

9 ³East China Mineral Exploration and Development Bureau, Nanjing 210007, China

10 *Correspondence to:* Xianghui Li (leeschhui@126.com)

11

12 **Abstract.** The magmatism (including volcanism) in East Asia (/ China) could provide key clues and age constrains for the
13 subduction and dynamical process of the Paleo-Pacific plate. Although lots of absolute isotope ages of extrusive rocks have
14 been published in the 1980s-2000s, large uncertainties and big errors prevent the magmatism in SE China from being well
15 understood. In this study, we investigate the zircon geochronology of extrusive rocks and tempo-spatial variations of the late
16 Mesozoic volcanism in Southeast (SE) China. We reported zircon U-Pb ages of new 48 extrusive rock samples in the
17 Shi-Hang tectonic zone. Together with the published data in recent decade, ages of 291 rock samples from ~ 40
18 lithostratigraphic units were compiled, potentially documenting a relatively complete history and spatial distribution of the
19 late Mesozoic volcanism in SE China. The results show that the extrusive rocks spanned ~ 95 Myr (177-82 Ma), but
20 dominantly ~ 70 Myr (160-90 Ma), within which the volcanism in the early Early Cretaceous (145-125 Ma) was the most
21 intensive and widespread eruption. We propose that these ages represent the intervals of the Yanshanian volcanism in SE
22 China. Spatially, the age geographic pattern of extrusive rocks shows that both the oldest and youngest age clusters occur in
23 coastal magmatic arc (eastern Zhejiang and Fujian), and the most intensive and widespread age group (145-125 Ma) occurs
24 in back arc / rifting basin (eastern Jiangxi, middle Zhejiang, and northern Guangdong), implying that the late Mesozoic
25 volcanism migrated northwesterly and subsequently retreated southeasterly. This volcanic migration pattern may imply that the
26 Paleo-Pacific plate subducted northwestward and the roll-back subduction did not begin until the Aptian (~ 125 Ma) of the
27 mid-Cretaceous.

28 **Keywords:** geochronology; tempo-spatial variation; volcanism; late Mesozoic; Southeast China

29

30 1. Introduction

31 It is generally believed that an Andean-type active continental margin had been developed during the late Mesozoic in
32 eastern Eurasia along which the Paleo-Pacific plate (PPP) subducted beneath the East Asia (e.g., Taylor and Hayes, 1983;
33 Faure and Natal'in, 1992; Charvet et al., 1994; Zhou and Li, 2000; Chen et al., 2005; Liu et al., 2017; Li SZ et al., 2019).
34 The subduction has exerted profound impacts in Southeast (SE) China (e.g., Taylor and Hayes, 1983; Zhou and Li, 2000; Li
35 CL et al., 2014; Li JH et al., 2014; Jiang YH et al., 2015; Liu et al., 2016;) and many other parts of East Asia (e.g.,
36 Stepashko, 2006; Wu et al., 2007; Choi and Lee, 2011; Zhang et al., 2011; Sun et al., 2013; 2015; Dong et al., 2016; Liu et
37 al., 2017), as indicated by the pervasive crustal deformation associated with the Yanshanian orogeny (e.g., Lapierre et al.,
38 1997; Li, 2000; Zhou and Li, 2000) and the widespread magmatism (e.g., Zhou et al., 2006; Sun et al., 2007). Obviously, the
39 study of the magmatism would help to constrain the process of the PPP subduction.

40 The late Mesozoic volcanism in SE China, as a response to the PPP subduction, has long attracted attention, and lots of
41 dating work has been carried out. However, different time intervals and various episodes / cycles / periods of the volcanism
42 have been proposed (e.g., Li et al., 1989; Feng et al., 1993; Zhang, 1997; Guo et al., 2012; Li CL et al., 2014; Liu et al., 2012,
43 2014, 2016; Jiang SH et al., 2015; Ji et al., 2018; Zhang et al., 2018; Yang et al., 2018; Zhang et al., 2019). The issue can be
44 attributed to: 1) the published ages were generally based on separate and often limited datasets that were commonly from
45 only several to a dozen of samples from a local region such as a mining field, or a province, or at most from a relatively wide
46 area of two neighboring provinces; 2) age data were obtained using different methods, by which, the Rb-Sr, K-Ar, and Ar-Ar
47 dating of bulk-dominated samples yielded ages with large uncertainties and big errors in the 1980s-1990s; 3) refined zircon
48 U-Pb ages of the volcanism have not been analyzed for the whole SE China.

49 It is essential to obtain spatially more comprehensive datasets from different parts of SE China and also temporally more
50 expanded datasets from sedimentary basin archives that can document the relatively complete volcanic history to achieve a
51 holistic understanding of the late Mesozoic volcanism and geodynamics in SE China.

52 In this study, we investigate the geochronology of extrusive rocks in the middle and northern Shi-Hang tectonic belt (SHTB.
53 e.g., Gilder et al., 1996; Jiang et al., 2011; Yang et al., 2012). The SHTB contains thick sedimentary strata, which are
54 interbedded with extrusive rocks, and thus has the advantage of providing a more complete stratigraphic archive that
55 preserves more complete and recognizable volcanic events. We also compile the published zircon U-Pb isotope
56 geochronological data of extrusive rocks from the entire SE China. Obviously, ages of the extrusive rocks can constrain the
57 geochronology of the initiation, evolution, and termination of the late Mesozoic volcanism in SE China. Specifically, we
58 analyze the temporal evolution and the geographical distribution of the late Mesozoic volcanism, which can indirectly help
59 date and better understand the slab subduction between the eastern Asian continent and the western PPP in East Asia (e.g.,
60 Gilder et al., 1991, 1996).

61 2. Geological setting

62 The South China Block comprises the Yangtze Block and Cathaysia Block. The Yangtze Block has an Archean to
63 Proterozoic basement, whereas the Cathaysia Block has a Proterozoic basement. Yangtze and Cathaysia blocks amalgamated
64 during the early Neoproterozoic Orogeny (e.g., Zhao and Cawood, 1999; Wang et al., 2006; Zheng and Zhang, 2007; Li et
65 al., 2009), forming the Jiangnan orogen. A cover sequence of marine strata from the late Neoproterozoic to the Paleozoic
66 was accumulated on the united South China Block that subsequently underwent the Caledonian orogeny (or the Guangxi
67 movement) in the early Paleozoic (e.g., Guo et al., 1989; Qiu et al., 2000; Charvet et al., 2010) and the Indosinian orogeny in
68 the early Mesozoic (e.g., Carter et al., 2001; Lepvrier et al., 2004).

69 The major Jiangshan-Shaoxing suture zone separating the Yangtze and Cathaysia blocks (e.g., Jiang et al., 2011; Yang et al.,

2012) had been reactivated during the Indosinian and Yanshanian movements (e.g., Wang et al., 2013). During the Yanshanian, the Andean-type convergent margin was developed along the SE China following the subduction of the PPP (e.g., Taylor and Hayes, 1983; Faure and Natal'in, 1992; Charvet et al., 1994; Zhou and Li, 2000; Chen et al., 2005; Liu et al., 2017; Li SZ et al., 2019). A series of NE-striking back-arc basins associated with widespread and large-scale magmatism were produced (e.g., Zhou and Li, 2000; Li and Li, 2007; Liu et al., 2014, 2016; Xie et al., 2017; Yang et al., 2017). Since the deposition in these basins was concomitant with volcanism, it is fairly common that the sedimentary successions are interbedded with volcanic rocks. On the basis of the abundance of volcanic rocks in the strata, these basins can be grouped into three types (Fig. 1): volcanic (-dominated), volcanic-sedimentary, and sedimentary (e.g., Chen et al., 2005; Shu et al., 2009). These three types of basins are roughly separated by two NE-striking fault zones: the Jiangshan-Shaoxing fault zone and the Zhenghe-Dapu fault zone (Fig. 1). The volcanic basins occur SE to the Zhenghe-Dapu fault zone and were formed on the magmatic arc (Lapierre et al., 1997) along the coastline, i.e., the Coastal zone (CZ). The volcanic-sedimentary basins occur in the SHTB confined between the two fault zones, and volcanic rocks are typically interbedded and / or intercalated with sedimentary strata, which had been constructed in the back arc / rifting basin (e.g., Gilder et al., 1991; Jiang et al., 2009; 2011). Nevertheless, the late Mesozoic volcanic rocks are almost absent east to the Yujiang-Yudu fault zone in sedimentary basins and western SHTB basins (Fig. 1).

The large-scale magmatism is evidenced by the occurrence of granitic plutons in both the SHTB and the CZ stretching over 1000 km along the coastal SE China. These granitic plutons intruded into the Precambrian basement and the overlying Paleozoic strata during the Middle Jurassic-Early Cretaceous (e.g., Jiang et al., 2011; Yang et al., 2012). The intrusions mainly occur as A-type and / or I-type granitic rocks, and together with huge volcanic rocks, strongly support the model of the western subduction of the PPP (e.g., Zhao et al., 2016; Jiang et al., 2011; Yang et al., 2012; Xie et al., 2017; Yang et al., 2017).

3. Material and methods

A total of 48 extrusive rock samples were collected from about 20 lithostratigraphic formations (supplementary data Table S1) in 11 basins / regions within the main SHTB to obtain new zircon U-Pb isotope ages (L1-L10 in Fig. 1; supplementary data Figs. S1-S3 and Table S1). The extrusive rock specimens are volcanic and pyroclastic rocks that are interbedded and intercalated with the sedimentary strata, in which sampling horizons and associated lithologies are marked in the supplementary data figures S4-S12. These samples were collected from volcanic layers in the main type sections of typical basins in SE China (supplementary data Fig. S4-S12). In general, 3-4 rock samples were taken at lower/base, middle and upper/top part when a lithostratigraphic unit has multiple volcanic horizons or a volcanic layer is over 100-200 m thick (see supplementary data Table S1). The locations of these samples were determined with a GPS device and are marked on the geological maps (supplementary data Figs. S1-S3 and Table S1).

Zircon grains were separated using the conventional heavy liquid and magnetic techniques. Single zircon grains were handpicked and mounted on adhesive tapes, embedded in epoxy resin, and then polished to about half to one-third of their thickness and photographed in both reflected and transmitted light. Cathodoluminescence (CL) images were taken at the State Key Laboratory for Mineral Deposits Research, School of Earth Sciences and Engineering, Nanjing University, to examine the internal structures of single zircon grains before U-Pb isotope analysis.

LA-ICP-MS, U-Th-Pb analyses of single zircon grains were performed on a Nd of YAG 213 laser ablation system (Agilent 7500a, New Wave Research, U.S.A.) coupled with VG PQ Excell ICP-MS, which is housed in the State Key Laboratory for Mineral Deposits Research, Nanjing University. General ablation time is ca. 60 s and the ablation pit diameter is at 25-35 μm . The ablation repetition rate is 5 Hz with the incident pulse energy of about 10-20 J/cm^2 . Calibrations of mass fractionation were made using the index sample GEMOC/GJ (608 Ma). In each experiment, a total of 11 to 21 zircon grains were

measured, among which 8 to 18 grains yield concordant age data. Prior to each experiment, the standard GJ-1 and Mud Tank samples were measured. Other measurements follow the methods described by Jackson et al. (2004). Analyses of Mud Tank sample yielded a weighted $^{206}\text{Pb}/^{238}\text{U}$ age of $726 \pm 10 \text{ Ma} - 737 \pm 5 \text{ Ma}$ (2σ), which is in good agreement with the recommended value (TIMS age = $732 \pm 5 \text{ Ma}$, Black and Gulson, 1978).

Data reduction, isotope ratio, age calculation, and Pb correction were conducted with the GLITTER software using Zircon 91500 as an external standard. Data processing and plotting were executed with the Isoplot 3.23 programs (Ludwig, 2001). The uncertainties of age results are quoted at 1σ confidence level, whereas errors for weighted mean ages are quoted at 2σ .

It is worth noting that those aged samples of mafic dykes, basalts and gabbros were not herein compiled for the analysis of volcanic temporal-spatial variation in SE China. This is because: 1) among the magmatic rocks, gabbros and basalts are rare, and diorites and andesites are even less common in South China (Zhou and Li, 2000), leading to a weak significance in statistic of the volcanic samples; 2) those published ages of the dykes, basalts and gabbros were mainly measured using different (Ar-Ar, K-Ar, Rb-Sr) isotopic methods (e.g., Li, et al., 1989; Chen et al., 2008b; Wang et al., 2008; Meng et al., 2012), likely causing chaos of real ages; 3) it is difficult to obtain a good isotopic age for mafic rocks, and particularly, the bulk (basalt) samples ages by K-Ar, Ar-Ar, and Rb-Sr are $\sim 10\text{-}20 \text{ Ma}$ younger than those by zircon U-Pb isotopes (Li et al., 2019); and 4) some basalts predominantly are of the Indosinian orogeny age, instead of the Yanshanian orogeny.

4. Results

4.1 Uncertainty of zircon U-Pb ages

It is necessary to first evaluate the uncertainty of the new age results and other cited age data. The uncertainty depends on three aspects, i.e. origin of zircon, precision, and accuracy (Schoene et al., 2013).

For the origin, all zircons used in this work were microscopically evaluated with CL to ensure that laser ablation positions of zircons are away from the nucleus, cracks, and inclusions. CL images manifest the growth rings. In the concordant 636 zircons of this work, 20 grains (3.1 %) are 0.1-1.0 in Th/U ratio, 615 (96.7 %) are 1.0-10.0 (Table 1). Th/U ratios of 3539 zircons can be available in the age data from published references. Together with published data and this work, 1766 zircon grains (42.3 %) are 0.1-1.0 in Th/U ratio, 2394 grains (57.3 %) are 1.0-10.0, 14 grains (0.3 %) are > 10.0 , and only one is less than 0.1 (Table 1). CL images and Th/U ratios of this work combined the collected data demonstrate that predominant ($> 99.9 \%$), if not all, zircons are magmatic origin.

Precision and accuracy uncertainties produced during LA-ICP-MS zircon U-Pb dating have been more and more concerned (e.g., Klötzli et al., 2009; Solari et al., 2010; Li et al., 2015) and come from multiple sources, including the isotopic ratio measurements, the fractionation factor calculation using an external standard, the common lead correction, the external standards, and the data reduction (Li et al., 2015). According to the suggested $\sim 4 \%$ (2σ) of precision and accuracy (Li et al., 2015), we used the $\sim 2 \%$ and $\sim 2\text{-}4 \%$ (1σ) to evaluate uncertainties of extrusive rock ages.

A total of 48 rock samples were respectively weighed in mean from 636 concordant zircon U-Pb ages in this work (supplementary data Table S1 and S2). In the samples, 46 (95.8 %) have a < 3 million years (Myr) error in 1σ , in which 36 (75 %) samples have < 2 Myr error in 1σ ; 41 samples (85.4 %) have $< 2.0 \%$ (error / age) deviation, and 7 (14.6 %) have 2-4 % deviation (Table 1). Similar percentages of sample error and age deviation are comparative with those single zircons analyzed in this work (Table 1).

For zircons from the published data, the literature often provides CL images of zircons showing quite similar nature in source and error. For the zircon U-Pb ages from the previous studies, we carefully examine the experiments described in the literature, re-analyze the concordant ages, and eliminate those that are not concordant and / or greater than $\sim 5 \%$ in age deviation (error / age) as well as ages with distinct inheritance, which were not discarded by the original authors. This scrutinizing procedure allows us to identify reliable U-Pb age data from 188 volcanic rock samples from the SHTB and from

103 volcanic rock samples from the CZ (supplementary data Table S2 and S3). Then, results show that in the combined 291 samples, 246 samples (85.5 % = 246/291) are < 2 Myr in 1 σ error of age and 39 (13.4 %) are 2-4 Myr; and 264 samples (90.7 %) are < 2.0 % age deviation and 25 (8.6 %) are 2-4 Myr deviation in age (Table 1). Closely, total concordant single zircons 4639 are similar in percentages of 1 σ error and age deviation with the weighed-mean age samples (Table 1). The above relatively low errors in 1 σ and deviation of age indicate that samples of both this and previous work have highly proportional age results (> ~ 95 %) with fine precision. Systematic biases often dominate uncertainty in comparisons between dating methods and between laboratories (Schoene et al., 2013). For measurements of our zircon samples, the internal systematic 2 σ error is less than 3 %, which has been verified by reproductive measurements of Mud Tank sample (see Section 3). These systematic biases were mostly met for those zircons from the references. Therefore, small internal systematic 2 σ errors allow our zircon date results to be a moderate accuracy in geochronological application. The internal systematic conditions are same for weighted mean dates of individual samples from both this and previous work (ref. and comp. to supplementary data Table S1-S3). Compiled zircons are predominantly single dates generally within less than 2 Myr in 1 σ errors (< 3 % biases) for the Late Jurassic – Early Cretaceous volcanic rocks. The dates are to great degree consistent with the biostratigraphy of pollens-spores, plants, ostracods, and conchostracans in the volcanic-sedimentary basins, SHTB (e.g., Chen and Shen, 1982; Sha, 1990; Jiang et al., 1993; Chen, 2000). In summary, the zircon origin and the age precision and accuracy indicate the sample weighed-mean ages have relatively low uncertainty and they are eligible for investigating the eruption geochronology of extrusive rocks in SE China.

4.2 U-Pb age spectra of extrusive rocks

Spot analyzing results of this work show that 48 samples have a wide range of (concordant $^{206}\text{Pb}/^{238}\text{U}$) weighed-mean ages from 162 Ma to 92 Ma (green histogram, Fig. 2a), from which two peaks of weighted mean ages are inconspicuously regressed as 133.3 ± 1.5 Ma and 97.2 ± 1.1 Ma, respectively (Fig. 2a). In addition, 636 concordant single zircons from the samples show similar wide age range (166 Ma to 92 Ma) with three age peaks (Fig. 2a. 135.87 ± 0.42 Ma, 124.71 ± 0.35 Ma, and 98.91 ± 0.57 Ma).

Combining our new results with the published age data from the main SHTB (e.g., Wu et al., 2011a, b; Wu and Wu, 2013; Liu et al., 2012, 2014, 2016; Li CL et al., 2014; Li JH et al., 2014; Ma et al., 2016; Wang et al., 2016; Shu et al., 2017. Locations M1-M22, Table S1 and Fig. 1) yields a similar age pattern (Fig. 2b). A total of 188 rock samples show that the weighed-mean age range from 177 Ma to 92 Ma with distinct age peak 136.11 ± 0.38 Ma and inconspicuous age peak 100.0 ± 1.0 Ma (Fig. 2b). Also, a total of 2593 single zircons from the SHTB show the concordant $^{206}\text{Pb}/^{238}\text{U}$ ages ranging from 180 Ma to 92 Ma with strong age peak 132.07 ± 0.17 Ma and weak peak 101.26 ± 0.23 Ma (Fig. 2b).

The published data of 103 rock samples from the CZ (for Locations N1-N21, see Fig. 1 and supplementary data Table S1 and S3. Chen et al., 2008; Li et al., 2009; Guo et al., 2012; Li CL et al., 2014; Liu et al., 2012, 2016; Zhang et al., 2018) show a wide weighed-mean ages ranging from 174 Ma to 82 Ma and three remarkable age peaks of 143.15 ± 0.82 Ma, 130.96 ± 0.87 Ma, and 98.13 ± 0.55 Ma (Fig. 2c), similar to those from the SHTB (comp. Fig. 2b and 2c). The 2046 single zircons from the 103 samples also display the same range of concordant $^{206}\text{Pb}/^{238}\text{U}$ ages (Fig. 2c; supplementary data Table S3) with two prominent age peaks (131.04 ± 0.32 Ma and 99.08 ± 0.32 Ma. Fig. 2c).

Further combined and optimized age data of 291 extrusive rock samples of over 40 lithostratigraphic units in both SHTB and CZ illustrate that sample weighed-mean ages mainly vary between 177 Ma and 82 Ma (Fig. 3). Of the ages, two peaks are at 132.86 ± 0.46 Ma (75 samples, 138-130 Ma, MSWD = 2.3) and 98.19 ± 0.47 Ma (25 samples, 100-96 Ma, MSWD = 1.14), respectively. The compilation of age data from all the 4639 concordant single zircons shows that the $^{206}\text{Pb}/^{238}\text{U}$ ages range between ~ 180 Ma and ~ 76 Ma with two age peaks at 132.90 ± 0.14 Ma and 99.86 ± 0.19 Ma (Fig. 3).

194 **5.1 Temporal evolution of volcanism**

195 The late Mesozoic extrusive rocks are widespread in SE China and their dating has been conducted extensively. In early
196 times, they have been roughly dated as the (Late) Jurassic and (to the Late) Cretaceous by the confinement of interbedded /
197 intercalated terrestrial fossil-bearing sedimentary strata, and the ages are quite crude. Later on, Rb-Sr, K-Ar, and Ar-Ar
198 dating of bulk-dominated samples yielded ages of ~ 150-65 Ma with large age uncertainties in the 1980s-1990s (e.g., Hu et
199 al., 1982; Li et al., 1989; Feng et al., 1993; Zhang, 1997), much younger than the earlier rough estimates, and ~ 10-20 Myr
200 younger than the zircon U-Pb isotope ages on average (Li et al., 2019).

201 In the recent decade, though zircon U-Pb age data of the igneous rocks have been reported, rock samples in individual
202 references were taken from separate locations resulting in different age interpretations of volcanic eruption in SE China, and
203 a relative concurrent viewpoint has not been reached. Multiple volcanic age durations are available at different locations or
204 regions, such as 145-129 Ma, 143-98 Ma, and 140-118 Ma in eastern and northwestern Zhejiang (Liu et al., 2014), 140-88
205 Ma and 136-129 Ma in southeastern (Liu et al., 2012) and central Zhejiang (Li JH et al., 2014), 168-95 Ma in northeastern
206 Guangdong and southeastern Fujian (Guo et al., 2012), 162-130 Ma from two locations in Fujian (Li et al., 2009), 160-99
207 Ma from northern Fujian (Liu et al., 2016), and 112-99 Ma from Zijingshan Mineral Field of Fujian (Jiang et al., 2013, 2015).
208 Obviously, these ages are incomplete and intermittent, and cannot individually reveal the age of volcanism in the entire SE
209 China.

210 To investigate the geochronology of extrusive rocks, we conducted zircon U-Pb age analysis in the SHTB and combined the
211 published data from both SHTB and CZ. Then relatively high precise and representative dating results are obtained in entire
212 SE China: the combined and optimized ages from 291 rock samples (4639 concordant zircons) range from ~ 177 Ma to ~ 82
213 Ma (mainly 160-90 Ma).

214 As we know, the U-Pb isotope ages of zircons represent the cease time of the crystalline zircon formation when volcanic
215 eruption, therefore, we propose that the age range above is an eligible representation for the duration of volcanism in SE
216 China. That means, the volcanism could have initiated at the late Toarcian (~ 177 Ma) of the late Early Jurassic and
217 terminated at the early Campanian (~ 82 Ma) of the Late Cretaceous, and it has a ~ 95 Myr duration, which shows little
218 discrepancy with those of the single zircon ages (Fig. 3). On the other hand, the volcanism occurred chiefly during the
219 interval of the Late Jurassic-early Late Cretaceous (160-90 Ma = 70 Myr) when only several samples with ages of pre-160
220 Ma and post-90 Ma are disregarded (e.g., Chen et al., 2007; Guo et al., 2012; Liu et al., 2012). When consider the
221 relationship of the magmatism to the Yanshanian origination, the above age range and duration (~ 177-82 Ma) probably
222 represent the time of the Yanshanian orogeny in East and SE Asia.

223 Then the temporal evolution scenario of the volcanism in SE China can be summarized as (Fig. 3): 1) during the latest Early
224 Jurassic (late Toarcian)-Latest Late Jurassic (~ 177-145 Ma), the volcanism was sporadic; 2) the early Early Cretaceous
225 (Berriasian-Barremian, ~ 145-125 Ma) volcanic eruption was the most intensive; 3) and the volcanism became fading during
226 the main mid-Cretaceous (Aptian-Turonian, ~ 125-92 Ma); 4) the volcanism almost ceased since then (~ 92-82 Ma). The
227 most extensively volcanic eruption episode (145-25 Ma) seems to correspond to the period of rapid increase in the magmatic
228 flux of both the Mid-ocean ridge and Large Igneous Provinces (Coffin & Eldholm, 1994) during the late Late Jurassic-early
229 Early Cretaceous (Fig. 4) although the relationship between them remains unclear.

230 It is noted that among the compiled single zircon U-Pb ages of extrusive rocks, the oldest one is from the Maonong
231 Formation in the Songyang Basin, southwestern Zhejiang. The weighted mean age is 177.4 ± 1.0 Ma for the sample MN01
232 (location M14. Liu et al., 2012). In addition, a weighted mean age of 180 ± 4 Ma from the same horizon (Chen et al., 2007)
233 has also been reported despite that the error is relatively large, up to 6-8 Myr.

234 Similarly, variable youngest ages of volcanic rocks are reported. The weighted-mean age 82.5 ± 1.0 Ma of the sample ZJ23

(location N2. Chen et al., 2008) from the Taozu section of eastern Zhejiang could be the youngest age. One zircon grain from the section is dated at 74 ± 0.6 Ma and five zircon grains yield concordant ages of 76 ± 0.6 Ma from the same sample (Table S3. Chen et al., 2008), suggesting that it is possible the termination of volcanism was ~ 5 Myr younger than 82.5 Ma. Two hiatuses volcanism at 128-122 Ma and 120-110 Ma were recently proposed in eastern Zhejiang (Liu et al., 2012), and volcanic reticence of 130-115 Ma was reported in northeastern Guangdong and southeastern Fujian (Guo et al., 2012. N17, N19, N20 in figure 1). Similar silence / inactiveness of volcanism seems happened in other parts of SE China. However, this volcanic silence is a gloss, and it would not have happened when we see all the late Mesozoic volcanism in SE China.

5.2 Spatial pattern of volcanism

Though it is well-known that the late Mesozoic magmatic rocks are widespread in SE China, the previous volcanic distributions are to some degree out of date as those ages contain large errors with low preciseness and accuracy by bulk isotope dating (e.g., Li et al., 1989; Wang et al., 2000; Zhou and Li, 2000; Chen et al., 2008b) and detailed age distribution patterns by precise age constraints have not been outlined yet. To delineate the spatial variation of the late Mesozoic volcanism in SE China that are refined by the zircon U-Pb geochronology, we sketched three distribution maps of extrusive rocks by the initial, peak, and terminal ages of volcanism (Fig. 5a, 5b, and 5c).

Firstly, we identified the initial ages of extrusive rocks. The initial age is defined as the earliest age of volcanic eruption in a location, a basin, and / or a region marked as capital letters L, M and N with numbers in figure 1. Three age boundaries ~ 163 Ma, ~ 145 Ma, and ~ 125 Ma are chosen to divide the initial ages into four intervals: 177-163 Ma, 163-145 Ma, 145-125 Ma, and < 125 (-94) Ma, ordinarily corresponding to the epochs of the Middle and Late Jurassic, the early and late Early Cretaceous, respectively. We used the boundary age 177 Ma as the earliest boundary within the first period of the volcanism because it could represent the initiation time of the first Yanshanian orogenic episode in SE China and the corresponding stratal boundary is marked by an unconformity (e.g., Yu et al., 2003; Shu et al., 2009). The boundary between the Upper Jurassic and the Lower Cretaceous is also represented by a widely observed unconformity (e.g., Yu et al., 2003; Shu et al., 2009) and the intensification of volcanism in SE China (Fig. 3). As there are fewer samples with ages of < 125 Ma and the age boundary at ~ 125 Ma marks the rapid waning of volcanism (Fig. 3), we designed the interval 125-94 Ma of volcanism as the latest initial age recognition.

Then, isolines ages are drawn by the boundary age 163 Ma, 145 Ma, and 125 Ma, separately. Interpolation ages are used to confine the zones when there are no exact ages same as the boundary age occur in the map. Plotting the initial ages in the geographical map shows four zones of initial volcanism in SE China (Fig. 5a). Zone 1 (Middle Jurassic, 177-163 Ma) marks areas where initial volcanic eruption locally occurs in the northernmost corner of Guangdong and neighboring southern corner of Fujian as well as northeastern corner of Fujian and at one location of southwestern Zhejiang (M14, Songyang, Liu et al., 2012). Zone 2 (Late Jurassic, 163-145 Ma) delineates areas where initial volcanic eruption occurs around Zone 1 in southern and northeastern Fujian with a much larger scope in southern Fujian than Zone 1. Zone 3 (early Early Cretaceous, 145-125 Ma) defines regions where initial volcanic eruption chiefly and largely extends in SE China, and mostly bounded in west of the volcanic area, extending along the eastern Jiangxi, northwestern Fujian, and middle Zhejiang (Fig. 5a). Zone 4 (late Early Cretaceous, 125-94 Ma) locally occupies eastern Zhejiang and limited southeastern Fujian (south of Fuzhou). Same zones can be also recognized in the map made from the single zircon U-Pb ages (comp. the supplementary data Fig. S13), supporting the zonations of the sample weighed-mean ages.

Secondly, the peak eruption age of extrusive rocks can be identified, which is defined as the main age of extensively volcanic eruption in a location, a basin, and / or a region marked with L, M and N with numbers in figure 1. Here we use 145 Ma, 125 Ma, and 100 Ma as three boundary ages to differentiate the most extensive volcanism in SE China. This is because the main ages are much younger than 145 Ma and few samples show ages younger than 100 Ma, for which the main age isolines are more readily made. Similarly, the corresponding age intervals confined by the boundary ages pertain to the

epochs of the Late Jurassic, the early and late Early Cretaceous, and early Late Cretaceous, respectively. Isolines of boundary ages are delineated by 145 Ma, 125 Ma, and 100 Ma and completed with interpolation ages when no exact ages in the transition zone. Four zones of peak volcanism are then shown in the geographical map, SE China (Fig. 5b). Zone 1 (Late Jurassic, 163-145 Ma) is the area where most intensively volcanic eruption occurred in southeastern and northeastern Fujian and locally at a place in southwestern Zhejiang (Fig. 5b). Zone 2 (early Early Cretaceous, 145-125 Ma) largely extends along the eastern Jiangxi, middle Zhejiang, northwestern Fujian, and northern Guangdong (Fig. 5b) and indicates widespread volcanism in SE China. Zone 3 (late Early Cretaceous, 125-100 Ma) occurs as a band in middle Zhejiang, southern Fujian, and northeastern Guangdong. Zone 4 (early Late Cretaceous, 100-76 Ma) locally distributes along Zone 3.

Thirdly, we use the terminal eruption age of extrusive rocks to represent the termination time of the last volcanism, which is helpful to distinguish the terminal volcanic distribution in SE China. The age boundaries and intervals are the same as the peak eruption. It is noted that only one age is older than 145 Ma in northeastern corner of Fujian and lots of samples are younger than 100 Ma.

With the confinement of boundary age 145 Ma, 125 Ma, and 100 Ma, age isolines are drawn separately, and interpolation method was used to confine the zones when there are no exact ages in the map. Four age zones of the terminal volcanism are recognized in the geographical map by the age isolines (Fig. 5c). Zone 1 (> 145 Ma) occurs in northeastern corner of Fujian due to only one location of the terminal age. Zone 2 (145-125 Ma) mainly occurs in eastern Jiangxi and banded boundary of northern Fujian; Zone 3 (125-100 Ma) largely distributes in the boundary region of eastern Jiangxi and western Fujian and in middle and southwestern Zhejiang. Zone 4 (100-83 Ma) widely appears in regions of the middle Fujian, eastern Zhejiang, and northern Guangdong. Similar zonations can be classified in the map sketched by the single zircon U-Pb ages (supplementary data Fig. S14), verifying the zones of the sample weighed-mean ages in SE China.

Zonations of initial, peak, and terminal volcanism indicate a distinct pattern of volcanic extrusion in SE China (Figs. 5): the oldest ages in the eastern SE China, the younger intensive age clusters in the western SE China and the youngest ones in eastern SE China again. Detailed distributional patterns can be observed: 1) the earliest appearance and earliest disappearance of extrusive rocks dominantly occur in southeastern and northeastern Fujian, where the magmatic arc was located (e.g., Lapiere et al., 1997); 2) the most widespread distribution of extrusive rocks is the most intensive volcanism age as 145-125 Ma in eastern Jiangxi, middle Zhejiang, and northern Guangdong, in which a back-arc / rifting basin was developed (e.g., Gilder et al., 1991; Jiang et al., 2009; 2011); 3) the latest appearance and latest disappearance mainly occur in eastern Zhejiang, eastern Fujian, and northern Guangdong.

With the observation of volcanism, two distributional patterns manifest: 1) the migration of the volcanism was from the northwestward to the southeastward, implying that the PPP could have been subducted northwesterly during the late Mesozoic time; 2) the first appearance (initial volcanism) area and the first disappearance (terminal volcanism) region are the same region, suggesting that a roll-back subduction of the PPP happened after ~ 125 Ma.

It is surprising that the zone 1 and / or 2 of volcanism look like thermal-dome patterns (Fig. 5) by exhumation and exposure that may be related to the regional magmatic intrusion, likely misleading the migration of volcanism. However, the distribution pattern is not dome-controlled because: 1) The data are derived from extrusive rocks, instead of intrusive rocks; 2) it is impossible that a crater is over 200-300 km wide in diameter; 3) lots of agglomerates representing craters were observed in a variety of strata at locations / basins out of Zone 1. For instance, these agglomerates are widespread in basins of western Zhejiang (L1-L4; M9-M14), eastern Jiangxi (L5-L7; M16-M18b), and western Fujian (L8-L10, M19-M22).

6. Conclusions

We analyzed weighed mean ages of 48 extrusive rock samples (total of 636 concordant single zircons) from ~ 20

lithostratigraphic units at 11 localities in the SHTB. Published ages of 243 rock samples (total of concordant 4003 zircons) from ~ 40 lithostratigraphic units in SE China are compiled and re-examined. Based on a total of refined 291 sample ages (4639 concordant zircon U-Pb ages) from this study and the published literatures, we propose that the late Mesozoic volcanism in SE China initiated at ~ 177 Ma (late Toarcian of the late Early Jurassic) and terminated at ~ 82 Ma (early Campanian of the Late Cretaceous), spanning an ~ 95 Myr interval (mainly ~ 70 Myr = 160-90 Ma), during which the 145-125 Ma (the early Early Cretaceous) volcanism is the most intensive and widespread magmatic eruption. These age range and span may represent the time of the Yanshanian magmatism in SE China. Isolines of initial, peak, and terminal volcanic ages are drawn to outline the geographic distribution of extrusive rocks in SE China. The volcanic extrusion age spatial change shows a distinct pattern of the late Mesozoic volcanism: both the oldest and youngest ages in eastern (coastal) Zhejiang and Fujian (magmatic arc), and the most intensive and widespread ages in eastern Jiangxi, middle Zhejiang and northern Guangdong (back arc / rifting basin), hundreds of kilometers away from the coast line. The geographical distribution pattern of the volcanic eruption ages indicates a migration process of magmatic extrusion in SE China and implies that a northwestern subduction of the Paleo-Pacific plate happened and a possible roll-back subduction did not begin until the Aptian (~ 125 Ma) of the mid-Cretaceous.

Acknowledgments

We thank Ke Cao, Sijing Liang, Yannan Ji, Sihe Wang for participating the field investigation. We are grateful to the reviewers for their helpful comments and constructive suggestions. This research was supported by National Key R & D Plan (Grant 2017YFC0601405), Natural Science Foundation of China (NSFC) projects 41372106 and 41672097, and National Basic Research Program of China (973 Project) 2012CB822003.

References cited

- Black, L. P., and Gulson, B. L.: The age of the Mud Tank carbonatite, Strangways Range, Northern Territory: BMR, J. Aust. Geol. Geophys., 3, 227-232, 1978.
- Carter, A., Roques, D., and Bristow, C.: Understanding Mesozoic accretion in Southeast Asia: Significance of Triassic thermotectonism (Indosinian orogeny) in Vietnam, *Geology*, 29, 211-214, 2001.
- Charvet, J., Lapierre, H., and Yu, Y. W.: Geodynamic significance of the Mesozoic volcanism of southeastern China, *J. SE Asi. Ear. Sci.*, 9, 387-396, 1994.
- Charvet, J., Shu, L. S., Faure, M., Choulet, F., Wang, B., Lu, H. F., and Le Breton, N.: Structural development of the Lower Paleozoic belt of South China: genesis of an intracontinental orogen, *J. Asi. Ear. Sci.*, 39, 309-330, 2010.
- Chen, C. H., Lee, C. Y., and Shinjo, R.: Was there Jurassic paleo-pacific subduction in South China?: constraints from ⁴⁰Ar-³⁹Ar dating, elemental and Sr-Nd-Pb isotopic geochemistry of the Mesozoic basalts, *Lithos*, 106, 83-92, 2008b.
- Chen, C. H., Lee, C. Y., Lu, H. Y., and Hseh, P. S.: Generation of Late Cretaceous silicic rocks in SE China: Age, major element and numerical simulation constraints, *J. Asi. Ear. Sci.*, 31, 479-498, 2008a.
- Chen, C. H., Lin, W., Lan, C. Y., and Lee, C. Y.: Geochemical, Sr and Nd isotopic characteristics and tectonic implications for three stages of igneous rock in the late Yanshanian (Cretaceous) orogeny, SE China, *Geol. Soc. Am., Special Paper*, 389, 237-248, 2005.
- Chen, P. J., and Shen, Y. B.: The Late Mesozoic conchostracan fossils in Jiangsu, Zhejiang and Anhui provinces, *Palaeont. Sin. China*, 161(17), 2-27 (in Chinese with English abstract), 1982.
- Chen, P. J.: The classification and correlation of non-marine Jurassic and Cretaceous of China: *Comment. J. Stratig.*, 24(2), 114-119 (in Chinese with English abstract), 2000.
- Chen, R., Xing, G. F., Yang, Z. L., Zhou, Y. Z., Yu, M. G., and Li, L. M.: Early Jurassic zircon SHRIMP U-Pb age of the

358 dacitic volcanic rocks in the southeastern Zhejiang Province determined firstly and its geological significances, *Geol. Rev.*,
359 53(1), 31-35 (in Chinese with English abstract), 2007.

360 Chen, W. F., Chen, P. R., Xu, X. S., and Zhang, M.: Geochemical characteristics of Cretaceous basaltic rocks in South China
361 and constraints on Pacific Plate subduction, *Sci. China (Series D)*, 48(12), 2104-2117, 2005.

362 Choi, T., and Lee Y. I.: Thermal histories of Cretaceous basins in Korea: Implications for response of the East Asian
363 continental margin to subduction of the Paleo-Pacific Plate, *Island Arc*, 20, 371-385, 2011.

364 Coffin, M. F., and Eldholm, O.: Large igneous provinces: Crustal structure, dimensions, and external consequences. *Rev.*
365 *Geophys.*, 32, 1-36, 1994.

366 Dong, Y., Ge, W. C., Yang, H., Xu, W. L., Zhang, Y. L., Bi, J. H., Liu, X. W.: Geochronology, geochemistry, and Hf isotopes
367 of Jurassic intermediate acidic intrusions in the Xing'an Block, northeastern China: Petrogenesis and implications for
368 subduction of the Paleo-Pacific oceanic plate. *J. Asi. Ear. Sci.*, 118, 11-31, 2016.

369 Faure, M., and Natal'in, B.: The geodynamic evolution of the eastern Eurasian margin in Mesozoic times, *Tectonophysics*,
370 208, 397-411, doi: 10.1016/0040-1951(92)90437-B, 1992.

371 Feng, Z. Z.: Mesozoic volcanism and tectonic environments in Fujian, *Reg. Geol. China*, 4(4), 311-316 (in Chinese with
372 English abstract), 1993.

373 Gilder, S. A., Gill, J., and Coe, R. S.: Isotopic and paleomagnetic constrains on the Mesozoic tectonic evolution of South
374 China. *J. Geophys. Res.*, 101, 16137-16154, 1996.

375 Gilder, S. A., Keller, G. R., and Luo, M.: Eastern Asia and the western Pacific timing and spatial distribution of rifting in
376 China, *Tectonophysics*, 197, 225-243, 1991.

377 Guo, F., Fan, W., Li, C., Zhao, L., Li, H., and Yang, J.: Multi-stage crust–mantle interaction in SE China: temporal, thermal
378 and compositional constraints from the Mesozoic felsic volcanic rocks in eastern Guangdong-Fujian provinces, *Lithos*, 150,
379 62-84, 2012.

380 Guo, L. Z., Shi, Y. S., Lu, H. F., Ma, R. S., Dong, H. G., and Yang, S. F.: The pre-Devonian tectonic patterns and evolution
381 of South China, *J. SE Asi. Ear. Sci.*, 3, 87-93, 1989.

382 Hu, H. G., Hu, S. L., Wang, S. S., and Zhu, M. The Jurassic and Cretaceous age of volcanic rocks on isotope dating, *Act*
383 *Geol. Sin.*, 56(4), 315-322 (in Chinese with English abstract), 1982.

384 Jackson, S. E., Pearson, N. J., Griffin, W. L., and Belousova, E. A.: The application of laser ablation-inductively coupled
385 plasma–mass spectrometry to in situ U/Pb zircon geochronology, *Chem. Geol.*, 211, 47-69, 2004.

386 Ji, W. B., Lin, W., Faure, M., Chen, Y., Chu, Y., Xu, Z. H.: Origin of the Late Jurassic to Early Cretaceous peraluminous
387 granitoids in the northeastern Hunan province (middle Yangtze region), South China: Geodynamic implications for the
388 Paleo-Pacific subduction, *J. Asi. Ear. Sci.*, 141, 174-193, 2017.

389 Jiang, S. H., Bagas, L., and Liang, Q. L.: New insights into the petrogenesis of volcanic rocks in the Shanghang Basin in the
390 Fujian Province, China, *J. Asi. Ear. Sci.*, 105, 48-67, 2015.

391 Jiang, S. H., Liang, Q. L., Bagas, L., Wang, S. H., Nie, F. J., and Liu, Y. F.: Geodynamic setting of the Zijinshan
392 porphyry-epithermal Cu-Au-Mo-Ag ore system, SW Fujian Province, China: constrains from the geochronology and
393 geochemistry of the igneous rocks, *Ore Geol. Rev.*, 53, 287-305, 2013.

394 Jiang, W. S., Zhen, J. S., Li, L. T., and Xu, K. D.: Study of the Cretaceous in Zhejiang, China, Nanjing, Nanjing University
395 Press, 1-42 (in Chinese with English summary), 1993.

396 Jiang, Y. H., Wang, G. C., Liu, Z., Ni, C. Y., Qing, L., and Zhang, Q.: Repeated slab advance-retreat of the Palaeo-Pacific
397 plate underneath SE China, *Intl. Geol. Re.*, 57, 472-491, 2015.

398 Jiang, Y. H., Zhao, P., Zhou, Q., Liao, S. Y., and Jin, G. D.: Petrogenesis and tectonic implications of Early Cretaceous
399 S-and A-type granites in the northwest of the Gan-Hang rift, SE China, *Lithos*, 121, 55-73, 2011.

400 Jiang, Y.H., Jiang, S.Y., Dai, B.Z., Liao, S.Y., Zhao, K.D., and Ling, H.F.: Middle to Late Jurassic felsic and mafic

magmatism in southern Hunan Province, Southeast China: implications for a continental arc to rifting, *Lithos*, 107, 185-204, 2009.

Klötzli U, Klötzli E, Günes Z, and Kosler, J.: Accuracy of laser ablation U-Pb zircon dating: Results from a test using five different reference zircons. *Geostand Geoanal Res*, 33, 5-15, 2009.

Lapierre, H., Jahn, B.M., Charvet, J., and Yu, Y. W.: Mesozoic felsic arc magmatism and continental olivine tholeiites in Zhejiang Province and their relationship with tectonic activity in SE China, *Tectonophysics*, 274, 321-338, 1997.

Lepvrier, C., Maluski, H., Maluski, H., Van Tich, V., Leyreloup, A., Thi, P. T., and Van Vuong, N.: The Early Triassic Indosinian orogeny in Vietnam (Truong Son Belt and Kontum Massif); implications for the geodynamic evolution of Indochina, *Tectonophysics*, 393(1-4), 87-118, 2004.

Li, C. L., Wang, Z. X., Wang, D. X., Cao, W. T., Yu, X. Q., Zhou, G. Z., and Gao, W. L.: Crust-mantle interaction triggered by oblique subduction of the Pacific plate: geochronological, geochemical, and Hf isotopic evidence from the Early Cretaceous volcanic rocks of Zhejiang Province, southeast China, *Intl. Geol. Rev.*, 56(14), 1732-1753, doi: 10.1080/00206814.2014.956347, 2014.

Li, J. H., Ma, Z. L., Zhang, Y. Q., Dong, S. W., Li, Y., Lu, M.A., and Tan, J. Q.: Tectonic evolution of Cretaceous extensional basins in Zhejiang Province, eastern South China: Structural and geochronological constraints, *Intl. Geol. Rev.*, 56(13), 1602-1629, doi: 10.1080/00206814.2014.951978, 2014.

Li, K. Y., Shen, J. L., and Wang, X. P.: Isotopic geochronology of Mesozoic terrestrial volcanic rocks in Zhejiang, Fujian and Jiangxi China, *J. Stratigr.*, 13(1), 1-13 (in Chinese with English abstract), 1989.

Li, S. Z., Suo, Y. H., Li, X. Y., Zhou, J., Santosh, M., Wang, P. C., Wang, G. Z., Guo, L. L., Yu, S. Y., Lan, H. Y., Dai, L. M., Zhou, Z. Z., Cao, X. Z., Zhu, J. J., Liu, B., Jiang, S. H., Wang, G., and Zhang, G. W.: Mesozoic tectono-magmatic response in the East Asian ocean-continent connection zone to subduction of the Paleo-Pacific Plate, *Earth-Sci. Rev.*, 192, 91-137, 2019.

Li, X. H.: Cretaceous magmatism and lithospheric extension in Southeast China. *J. Asi. Ear. Sci.*, 18, 293-305, 2000.

Li, X. H., Liu, X. M., Liu, Y. S., Su, L., Sun, W. D., Huang, H. Q., and Yi, K.: Accuracy of LA-ICPMS zircon U-Pb age determination: An inter-laboratory comparison, *Sci. China (Ear. Sci.)*, 58, 1722-1730, doi: 10.1007/s11430-015-5110-x, 2015.

Li, X. H., Zhang, C. K., Li, Y. X., Wang, Y., and Liu, L.: Refined chronostratigraphy of the late Mesozoic terrestrial strata in South China and its tectono-stratigraphic evolution, *Gond. Res.*, 66, 143-167, 2019.

Li, Z. X., and Li, X. H.: Formation of the 1300-km-wide intercontinental orogen and postorogenic magmatic province in Mesozoic South China: A flat-slab subduction model, *Geology*, 35, 179-182, 2007.

Liu, K., Zhang, J. J., Wilde, S. A., Zhou, J. B., Wang, M., Ge, M. H., Wang, J. M., and Ling, Y. Y.: Initial subduction of the Paleo-Pacific Oceanic plate in NE China: Constraints from whole-rock geochemistry and zircon U-Pb and Lu-Hf isotopes of the Khanka Lake granitoids, *Lithos*, 274-275, 254-270, 2017.

Liu, L., Xu, X. S., and Xia, Y.: Asynchronizing paleo-Pacific slab rollback beneath SE China: Insights from the episodic Late Mesozoic volcanism, *Gond. Res.*, 37, 397-407, 2016.

Liu, L., Xu, X. S., and Xia, Y.: Cretaceous Pacific plate movement beneath SE China: Evidence from episodic volcanism and related intrusions, *Tectonophysics*, 614, 170-184, 2014.

Liu, L., Xu, X. S., and Zou, H. B.: Episodic eruptions of the Late Mesozoic volcanic sequences in southeastern Zhejiang, SE China: petrogenesis and implications for the geodynamics of paleo-Pacific subduction, *Lithos*, 154, 166-180, 2012.

Ludwig, K. R.: *Squid 1.02: A User's Manual (2)*, Berkeley Geochron. Centre, Special Publication, 1-19, 2001.

Ma, Z. L., Li, J. H., Zhang, Y. Q., Dong, S. W., Song, C. Z., and Li, Y.: Geochronological and structural constraints on the lithostratigraphic units of the Lishui Basin, southeastern China, *Geol. China*, 43(1), 56-71 (in Chinese with English abstract), 2016.

Meng, L. F., Li, Z. X., Chen, H. L., Li, X. H., and Wang, X. C.: Geochronological and geochemical results from Mesozoic basalts in southern South China Block support the flat-slab subduction model, *Lithos*, 132-133, 127-140, 2012.

Qiu, Y. M., Gao, S., McNaughton, N. J., Groves, D. I., and Ling, W. L.: First evidence of N3.2 Ga continental crust in the Yangtze Craton of South China and its implications for Archean crustal evolution and Phanerozoic tectonics, *Geology*, 28(1), 11-14, 2000.

Schoene, B., Condon, D. J., Morgan, L., and McLean, N.: Precision and Accuracy in Geochronology, *Elements*, 9, 19-24, doi:10.2113/gselements.9.1.19, 2013.

Sha, J. G. *Plicatounio* from Hekou Formation of Hekou basin, Ninghua, Fujian, with discussion on classification of Plicatounionidae, *Acta Palaeont. Sin.*, 29(4), 472-489 (in Chinese with English abstract), 1990.

Shu, L. S., Zhou, X. M., Deng, P., Wang, B., Jiang, S. Y., Yu, J. H., and Zhao, X. X.: Mesozoic tectonic evolution of the Southeast China Block, New insights from basin analysis, *J. Asi. Ear. Sci.*, 34, 376-391, 2009.

Shu, X., Yang, S. Y., Jiang, S. Y., and Ye, M.: Petrogenesis and geodynamic setting of Early Cretaceous felsic rocks in the Gan-Hang Belt, Southeast China: Constraints from geochronology and geochemistry of the tuffs and trachyandesitic rocks in Shengyuan volcanic Basin, *Lithos*, 284-285, 691-708, 2017.

Solari, L. A., Gómez-Tuena, A., Bernal, J. P., Pérez-Arvizu, O., and Tanner, M.: U-Pb zircon geochronology with an integrated LA-ICP-MS microanalytical workstation: Achievements in precision and accuracy, *Geostand Geoanal Res*, 34, 5-18, 2010.

Stepashko, A. A.: The Cretaceous Dynamics of the Pacific Plate and Stages of Magmatic Activity in Northeastern Asia, *Geotectonics*, 40(3), 225-235, 2006.

Sun, M. D., Chen, H. L., Zhang, F. Q., Wilde, S. A., Dong, C. W., and Yang, S. F.: A 100 Ma bimodal composite dyke complex in the Jiamusi Block, NE China: An indication for lithospheric extension driven by Paleo-Pacific roll-back, *Lithos*, 162, 317-330, 2013.

Sun, M. D., Xu, Y. G., Wilde, S. A., and Chen H. L.: Provenance of Cretaceous trench slope sediments from the Mesozoic Wandashan Orogen, NE China: Implications for determining ancient drainage systems and tectonics of the Paleo-Pacific, *Tectonics*, 34, 1269-1289, doi:10.1002/2015TC003870, 2015.

Sun, W. D., Ding, X., Hu, Y. H., and Li, X. H.: The golden transformation of the Cretaceous plate subduction in the west Pacific, *Earth-Planet. Sci. Let.*, 262, 533-542, 2007.

Taylor, B., and Hayes, D.E.: Origin and history of the South China Sea Basin: in Hayes, D. E., Ed., *The Tectonic and Geologic Evolution of Southeast Asian Seas and Islands: Part 2*, Am. Geophys. Union Geophys. Monogr., 27, 23-56, 1983.

Wang, D. Z., Zhou, J. C., Qiu, J. S., and Fan, H. H.: Characteristics and petrogenesis of late Mesozoic granitic volcanic-intrusive complexes in southeastern China, *Geol. J. China Uni.*, 6(4), 487-798 (in Chinese with English abstract), 2000.

Wang, G. C., Jiang, Y. H., Liu, Z., Ni, C. Y., Qing, L., Zhang, Q., and Zhu, S. Q.: Multiple origins for the Middle Jurassic to Early Cretaceous high-K calc-alkaline I-type granites in northwestern Fujian province, SE China and tectonic implications, *Lithos*, 246-247, 197-211, 2016.

Wang, X. L., Zhou, J. C., Qiu, J. S., Zhang, W. L., Liu, X. M., and Zhang, G. L.: LA-ICPMS U–Pb zircon geochronology of the Neoproterozoic igneous rocks from Northern Guangxi, South China: implications for tectonic evolution, *Precambrian Res.*, 145 (1-2), 111-130, 2006.

Wang, Y. J., Fan, W. M., Cawood, P. A., Li, S. Z.: Sr–Nd–Pb isotope constraints on multiple mantle domains for Mesozoic mafic rocks beneath the South China Block hinterland, *Lithos* 106, 297-308, 2008.

Wang, Y. J., Fan, W. M., Zhang, G. W., and Zhang, Y. H.: Phanerozoic tectonics of the South China Block: Key observations and controversies, *Gond. Res.*, 23, 1273-1305, doi: 10.1016/j.gr.2012.02.019, 2013.

Wu, F., Yang, J., Lo, C., Wilde, S. A., Sun, D., and Jahn, B.: The Heilongjiang Group: a Jurassic accretionary complex in the

487 Jiamusi Massif at the western Pacific margin of northeastern China, *Island Arc*, 16, 156-172, 2007.

488 Wu, J. H., Liu, F. Y., and Liu, Sh.: SHRIMP U-Pb Zircon Age of Late Mesozoic Trachyte in Xiajiang—Guangfeng and
489 Sannan (Quannan, Dingnan and Longnan)—Xunwu Volcanic Belts, *Geol. Rev.*, 57(1), 125-132 (in Chinese with English
490 abstract), 2011a.

491 Wu, J. H., Xiang, Y. X., and Liu, S.: Wuyi Group of southern Jiangxi and its geological age, *J. Stratigr.*, 35(2), 200-208 (in
492 Chinese with English abstract), 2011b.

493 Wu, J., and Wu, J. H.: Shuangfengling formation in Jiangxi and its geological age, *J. East China Inst. Techn.*, 36, 17-24 (in
494 Chinese with English abstract), 2013.

495 Xie, J. C., Fang, D., Xia, D., Li, Q. Z., and Sun, W. D.: Petrogenesis and tectonic implications of late Mesozoic granitoids in
496 southern Anhui Province, southeastern China, *Intl. Geol. Rev.*, 59(14), 1804-1826, doi: 10.1080/00206814.2017.1297964,
497 2017.

498 Yang, J. B., Zhao, Z. D., Hou, Q. Y., Niu, Y. L., Mo, X. X., Sheng, D., and Wang, L. L.: Petrogenesis of Cretaceous (133–84
499 Ma) intermediate dykes and host granites in southeastern China: Implications for lithospheric extension, continental crustal
500 growth, and geodynamics of Palaeo-Pacific subduction, *Lithos*, 296-299, 195-211, 2018.

501 Yang, S. Y., Jiang, S. Y., Zhao, K. D., Jiang, Y. H., Ling, H. F., and Luo, L.: Geochronology, geochemistry and tectonic
502 significance of two Early Cretaceous A-type granites in the Gan-Hang Belt, Southeast China, *Lithos*, 150, 155-170, 2012.

503 Yang, Y. L., Ni, P., Yan, J., Wu, C. Z., Dai, B. Z., and Yu, Y. F.: Early to late Yanshanian I-type granites in Fujian Province,
504 SE China: Implications for the tectonic setting and Mo mineralization, *J. Asi. Ear. Sci.*, 137, 194-219, 2017.

505 Yu, X. Q., Shu, L. S., Deng, P., Wang, B., and Zhu, F. P.: The sedimentary features of the Jurassic-Tertiary terrestrial strata in
506 southeast China, *J. Stratigr.*, 27(3), 254-263 (in Chinese with English abstract), 2003.

507 Zhang, B., Guo, F., Zhang, X. B., Wu, Y. M., Wang, G. Q., and Zhao, L.: Early Cretaceous subduction of Paleo-Pacific
508 Ocean in the coastal region of SE China: Petrological and geochemical constraints from the mafic intrusions, *Lithos*,
509 334-335, 8-24, 2019.

510 Zhang, C., Ma, C. Q., Liao, Q. N., Zhang, J. Y., and She, Z. B.: Implications of subduction and subduction zone migration of
511 the Paleo-Pacific Plate beneath eastern North China, based on distribution, geochronology, and geochemistry of Late
512 Mesozoic volcanic rocks, *Intl. J. Earth Sci. (Geol Rundsch)*, 100, 1665-1684, 2011.

513 Zhang, J. H., Yang, J. H., Chen, J. Y., Wu, F. Y., and Wilde, S. A.: Genesis of late Early Cretaceous high-silica rhyolites in
514 eastern Zhejiang Province, southeast China: A crystal mush origin with mantle input, *Lithos*, 296-299, 482-495, 2018.

515 Zhang, L. M.: The Jurassic-Cretaceous boundary in the Zhejiang-Fujian-Jiangxi region, *Geol. Rev.*, 43(1), 25-31 (in Chinese
516 with English abstract), 1997.

517 Zhao, G. C., and Cawood, P. A.: Tectonothermal evolution of the Mayuan assemblage in the Cathaysia Block: new evidence
518 for Neoproterozoic collisional-related assembly of the South China craton, *Am. J. Sci.*, 299, 309-339, 1999.

519 Zhao, J. L., Qiu, J. S., Liu, L., and Wang, R. Q.: The Late Cretaceous I- and A-type granite association of southeast China:
520 Implications for the origin and evolution of post-collisional extensional magmatism, *Lithos*, 240-243, 16-33, doi:
521 org/10.1016/j.lithos.2015.10.018, 2016.

522 Zheng, Y. F., and Zhang, S. B.: Formation and evolution of Precambrian continental crust in South China, *Chinese Sci. Bull.*,
523 52, 1-12, 2007.

524 Zhou, X. M., and Li, W. X.: Origin of Late Mesozoic igneous rocks in southeastern China: implications for lithosphere
525 subduction and underplating of mafic magmas, *Tectonophysics*, 326, 269-287, 2000.

526 Zhou, X. M., Sun, T., Shen, W. Z., Shu, L. S., Niu, Y. L.: Petrogenesis of Mesozoic granitoids and volcanic rocks in South
527 China: a response to tectonic evolution, *Episodes*, 29(1), 26-33, 2006.

528

530 Table 1 Percentages of single zircons and rock samples in 1σ error (Myr), error/age ratio, and Th/U ratio of the late
531 Mesozoic extrusive rocks in SE China

Sources	<i>I</i>	<i>2</i>	1σ error						Error / age						³ (Th/U)	Th/U		
			Age (Myr)	<i>3</i>	%	Age (Myr)	<i>3</i>	%	Ratio	<i>3</i>	%	Age (Myr)	<i>3</i>	%		Ratio	<i>3</i>	%
This work in SHTZ	636	48	<3	570	89.6	<2	46	95.8	0-3	581	91.4	<2	41	85.4	636	<0.1	1	0.2
			3-5	63	9.9	2-4	2	4.2	3-5	50	7.9	2-4	7	14.6		0.1-1.0	20	3.1
			>5	3	0.5	>4			>5	5	0.8	>4				1.0-10	615	96.7
Composed in SHTZ	2593	188	<3	2066	79.7	<2	153	81.4	0-3	2212	85.3	<2	168	89.4	2503	<0.1	1	0.0
			3-5	441	17.0	2-4	31	16.5	3-5	348	13.4	2-4	18	9.6		0.1-1.0	945	37.8
			>5	86	3.3	>4	4	2.1	>5	33	1.3	>4	2	1.1		1.0-10	1543	61.6
Composed in SHTZ + CZ	4639	291	<3	3543	76.4	<2	246	84.5	0-3	3798	81.9	<2	264	90.7	4175	<0.1	1	0.0
			3-5	898	19.4	2-4	39	13.4	3-5	769	16.6	2-4	25	8.6		0.1-1.0	1766	42.3
			>5	198	4.3	>4	6	2.1	>5	73	1.6	>4	2	0.7		1.0-10	2394	57.3

Notes: Numbers of evaluated zircon grains differ from sources in U-Pb age and Th/U ratio due to unavailability of some original dada. CZ, Coastal zone; SHTC, Shi-Hang tectonic zone. 1, Con-cordant zircon Number; 2, Rock Sample number; 3, Zircon number

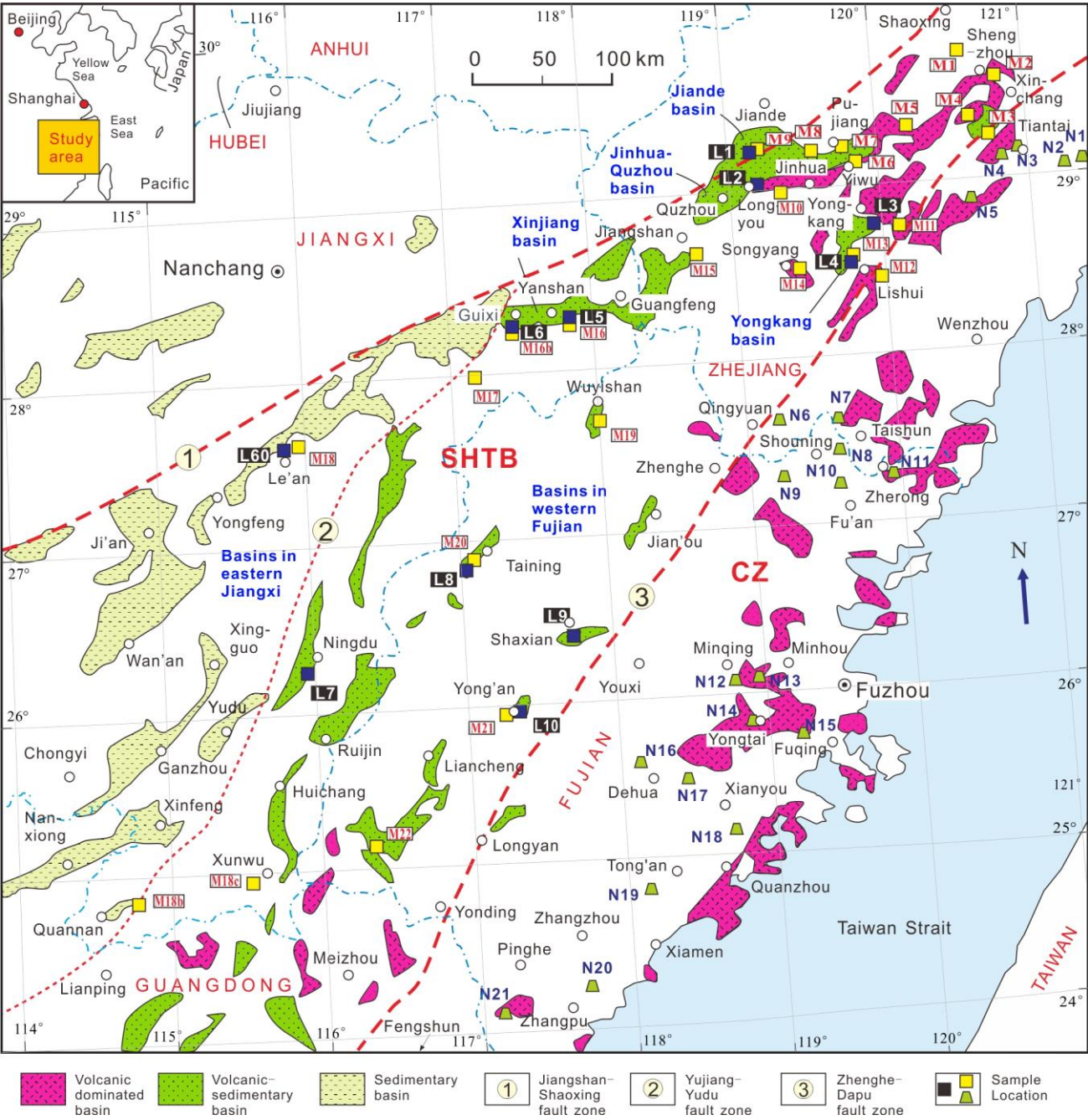


Figure 1 Geological map sketch of South China showing tectonic and basin zonation of the upper Mesozoic and sample locations (map simplified after Shu et al., 2009). In SHTB (Shi-Hang tectonic belt), dark blue squares with white capital letter L + numbers within black rectangles mark the sampling locations of this study (supplementary data figures S1, S2, and S3), and yellow squares with red capital letter M + numbers within white rectangles indicate sampling locations of previous studies (supplementary data Table S1 and S2). In CZ (Coastal Zone), green trapezoids with bold capital letter N + numbers are sample locations of previous studies (supplementary data Table S1 and S3).

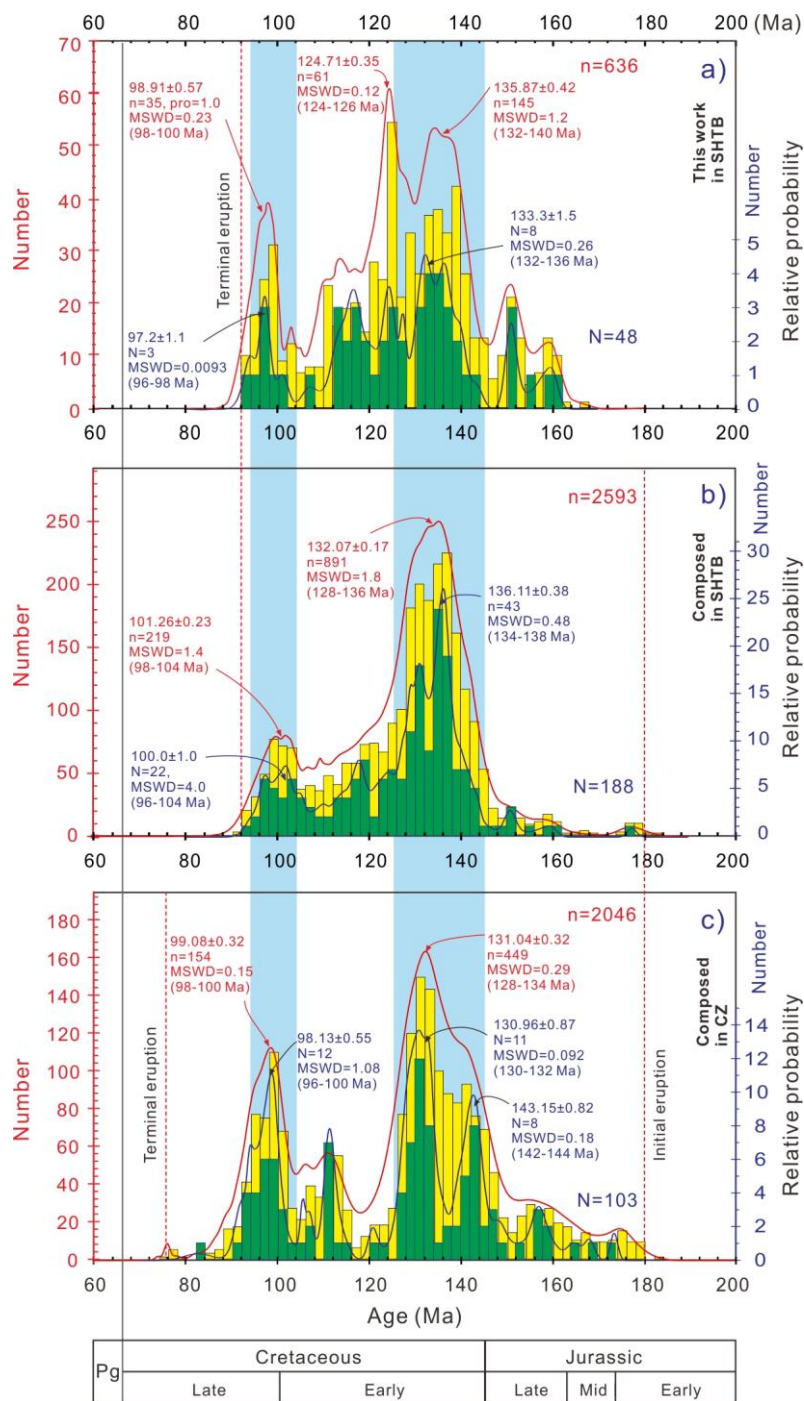


Figure 2 Relative probability and histogram diagrams of concordant zircon U-Pb isotope and sample weighed-mean ages of extrusive rocks from SE China (details see in supplementary data Table S1, S2, and S3). a), this study in SHTB; b), combined this and previous studies in SHTB; c), published data in CZ. N = number of rock samples, n = total number of zircon grains.

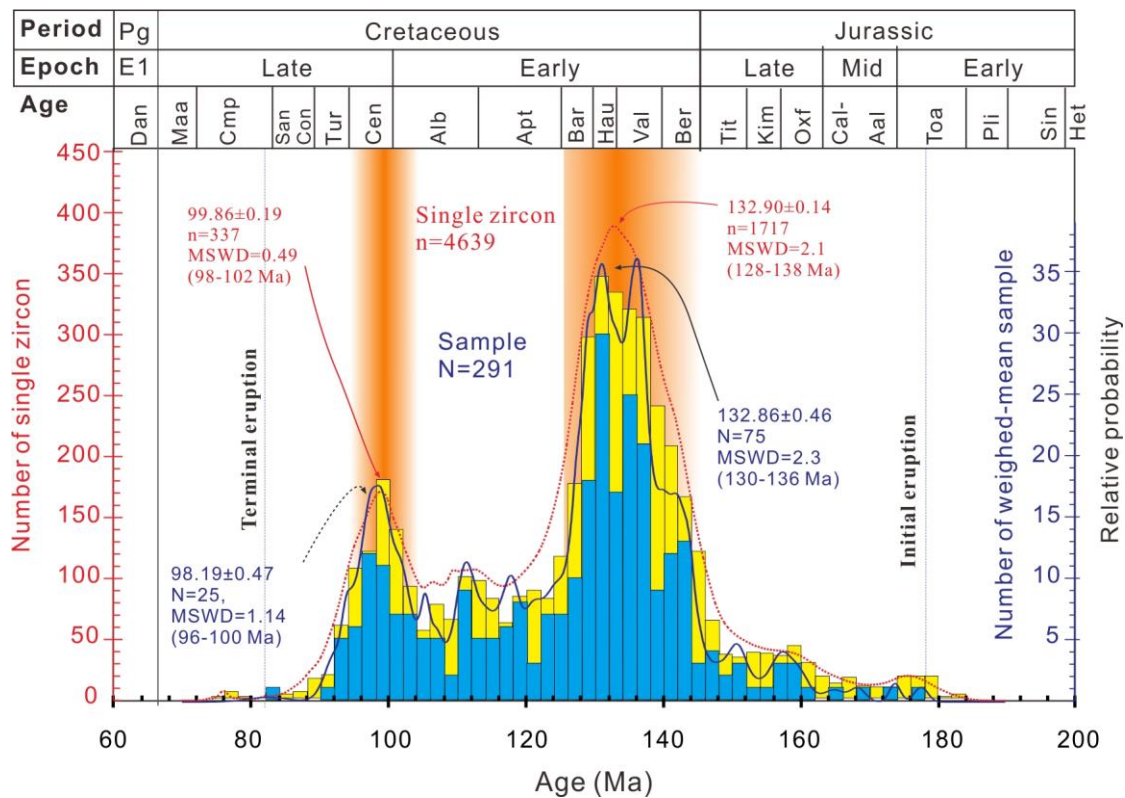


Figure 3 Diagram showing U-Pb isotope age relative probability and histogram of both single zircon and individual sample weighed-mean zircons from all extrusive rock samples in SE China. N = number of rock samples, n = total number of zircon grains.

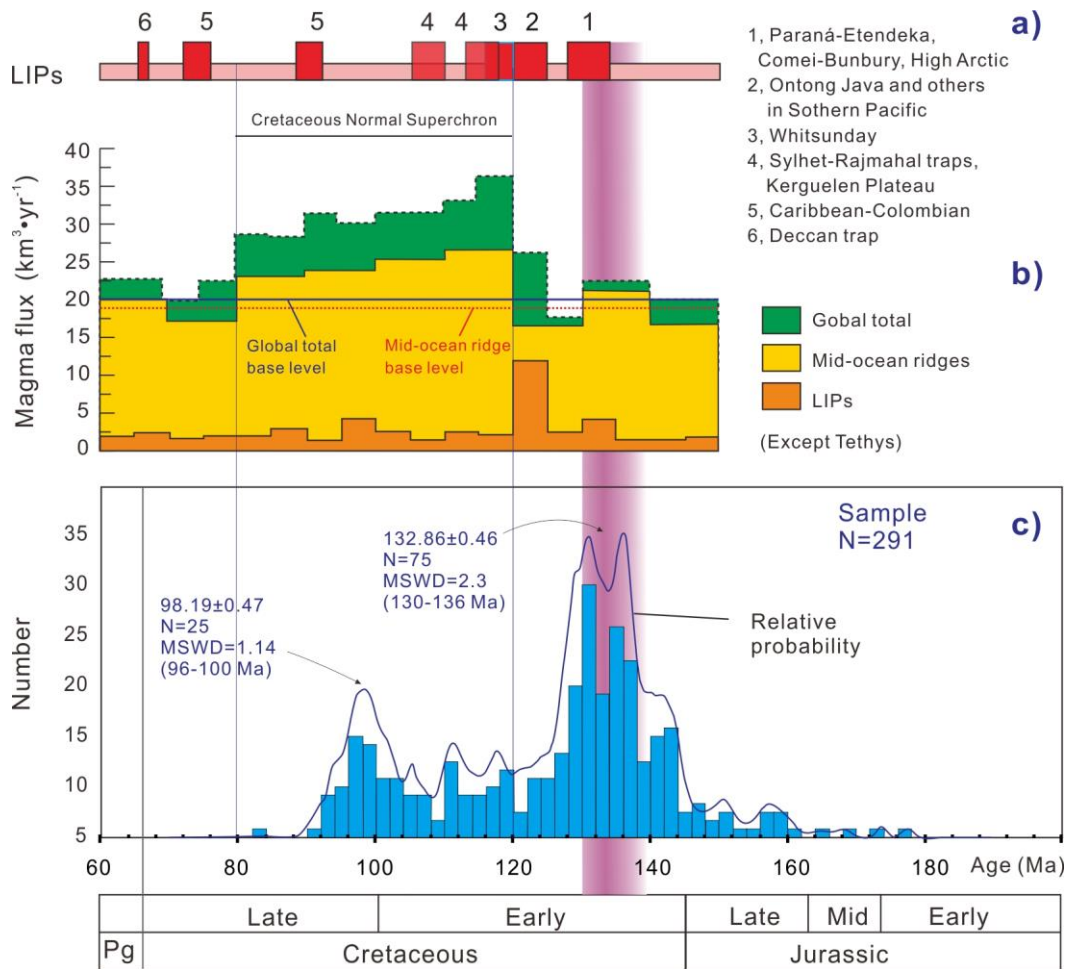


Figure 4 Diagram showing age ranges of volcanism in SE China and correlations with the global Large Igneous Provinces (LIPs) and magmatic flux. **a**, age range of the Cretaceous LIPs (summary see Coffin & Eldholm, 1994); **b**, magma flux of the Cretaceous LIPs, mid-ocean ridges, and (except Tethys) global total (Coffin & Eldholm, 1994); **c**, age range of the volcanism with histogram and relative probability and SE China.

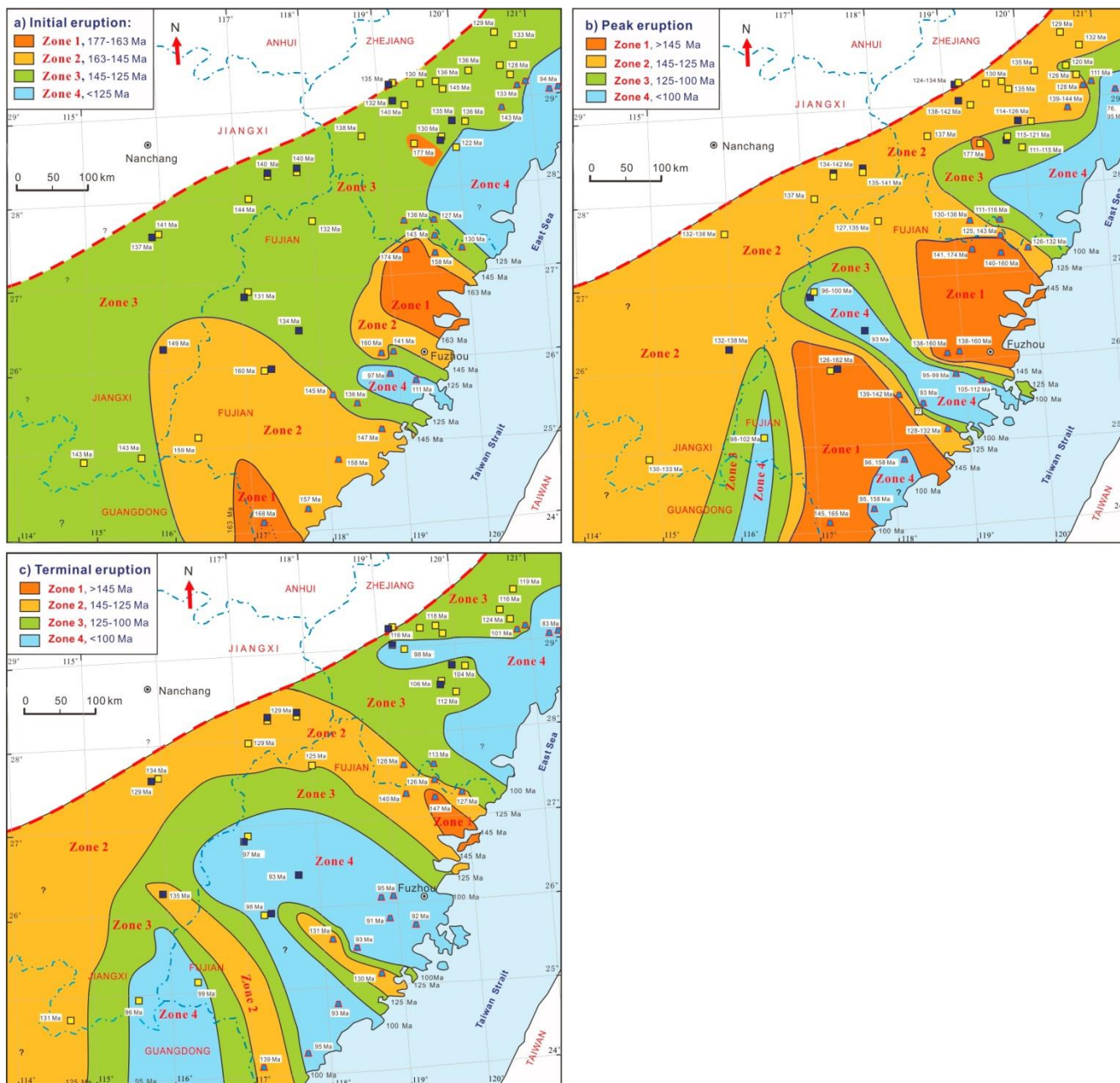


Figure 5 Sketch maps showing zonation of the late Mesozoic volcanism by age in SE China. Age within white rectangles is the eruption time at a location or in a basin/region. Names of color squares and trapezoids refer to Fig. 1. a), zonation of initial eruption ages; b) zonation of peak eruption ages; c) zonation of terminal eruption ages.